Magnetic scattering and spin-orbit coupling induced magnetoresistance in nonmagnetic heavy metal and magnetic insulator bilayer systems

B. F. Miao, L. Sun, D. Wu, C. L. Chien, and H. F. Ding

Phys. Rev. B **94**, 174430 — Published 21 November 2016

DOI: 10.1103/PhysRevB.94.174430

Magnetic Scattering and Spin-Orbit Coupling Induced Magnetoresistance in Nonmagnetic Heavy Metal and Magnetic Insulator Bilayer System

B. F. Miao[1], L. Sun[1,2], D. Wu[1,2], C. L. Chien[3], and H. F. Ding[1,2]*

[1]*National Laboratory of Solid State Microstructures and Department of Physics, Nanjing University, 22 Hankou Road, Nanjing 210093, P. R. China*

[2]*Collaborative Innovation Center of Advanced Microstructures, Nanjing University, 22 Hankou Road, Nanjing 210093, P. R. China*

[3]*Department of Physics and Astronomy, Johns Hopkins University, Baltimore, Maryland 21218, USA*

*Corresponding author: hfding@nju.edu.cn

We report on the experimental study of the angular dependent magnetoresistance (MR) of heavy metal/ferromagnetic insulator bilayer structures. Through altering the relative composition in heavy metal $Pt_{\delta}Ta_{1-\delta}$ alloy, we continuously tune its spin Hall angle from positive, crossing zero, to negative and study its impact on the MR. Most notably, both spin Hall effect and MR disappear simultaneously in $Pt_{0.32}Ta_{0.68}$(3 nm)/YIG when the effective spin Hall angle vanishes, evidencing the essential role of spin-orbit coupling in heavy metal for the MR. By introducing Fe impurities, we further identify that magnetic scattering is also essential to induce the MR in Pt/Fe-doped SiO_2 at large magnetic field, where the MR ratio increases monotonically with doping level.

The phenomena of magnetoresistance (MR), the change of electrical resistance of a material in response to an external magnetic field, such as giant magnetoresistance (GMR) [1, 2], tunneling magnetoresistance (TMR) [3, 4], colossal magnetoresistance (CMR) [5] have been major discoveries in condensed matter physics. Equally impressive, GMR, TMR, and anisotropic magnetoresistance (AMR) [6] discovered much earlier, have led to important technologies in non-volatile recording and magnetic sensing. All of the above mentioned MRs occur with the electric current passing through ferromagnetic (FM) materials or nanostructures. Of those the simplest MR is the AMR in polycrystalline FM materials. It possesses the characteristics of $R=R_{||}-\Delta R\sin^2\phi$, where $R_{||}$ and R_T are the longitudinal resistance ($\boldsymbol{M}||I$) and the transverse resistance R_T ($\boldsymbol{M}\perp I$), respectively, ϕ is the angle between magnetization ($\boldsymbol{M}$) and the electric current (I) both are in the film plane, and $\Delta R=R_{||}-R_T$ [7, 8]. When the magnetization is orientated in the out-of-plane direction by a magnetic field, one measures the same resistance $R_\perp\approx R_T$. In AMR, most often $\Delta R>0$, namely $R_{||}>R_\perp\approx R_T$.

Recently, an intriguing MR has been observed in Pt/YIG bilayer structure. Although electrons pass through only the non-magnetic Pt layer, its resistance unexpectedly reflects the magnetization direction of the underlying but insulating YIG substrate [9, 10]. The MR behavior of Pt/YIG with an in-plane field is identical to the well-known AMR, with $R_{||} > R_T$ and a $\sin^2\phi$ angular dependence. However, it exhibits a totally different behavior under an out-of-plane magnetic field. At room temperature, $R_{||}\approx R_\perp>R_T$, in sharp contrast to the AMR with $R_{||}>R_\perp\approx R_T$ [11-14]. This is a new type MR with a characteristic that are

clearly discernible from those of all other known MRs. Phenomenally, it can be described by $R=R_{||}-\Delta R m_y^2$, where m_y is the y component of YIG magnetization direction.

In order to explain this unique angular dependence, a theoretical model termed spin Hall magnetoreistance (SMR) has been proposed [12, 15]. In the SMR framework, the spin current (spin index $\boldsymbol{\sigma}$) generated from spin Hall effect (SHE) in Pt has different reflection coefficients at the Pt-YIG interface depending on the relative orientation of spin index $\boldsymbol{\sigma}$ and YIG magnetization $\boldsymbol{M}$ [16, 17]. The reflected spin current in Pt, in turn, induces an additional charge current via the inverse spin Hall effect (ISHE) [18]. Thus, changing the relative angle between $\boldsymbol{M}$ and $\boldsymbol{\sigma}$ (along the y direction) modulates the resistance and results in an angular dependence with $R_{||}\approx R_{\perp}>R_{\mathrm{T}}$. The MR effect therefore should saturate when the YIG magnetization is aligned by a magnetic field. Experimentally, however, the value of ΔR of Pt/YIG has been observed to increase with magnetic field unabated even after the saturation of the underlying YIG [19, 20]. Similar behavior has also been reported in the Pd/YIG system [21]. This is in sharp contrast to the theoretical prediction. By altering the Pt-YIG interface, crucial for pure spin current, it was demonstrated that MR in Pt/YIG contains two contributions, both give the same angular dependence with $R_{||}\approx R_{\perp}>R_{\mathrm{T}}$ at room temperature. The MR at low field can be generally understood by the SMR model; The physical mechanism of the MR at high field, however, remains a hot debate. It was initially associated with the induced moment in Pt-YIG interface due to magnetic proximity effect [9, 10, 19]. On the other hand, Vélez *et.al.*, attributed the high field MR in Pt/YIG to the Hanle effect in Pt film, even without the presence of magnetic material [20, 22]. To reveal the physical origin of this unique

high field MR in Pt/YIG and similar systems, comprehensive experimental evidence is highly required.

In this work, we present a systematic study of MR in $Pt_{\delta}Ta_{1-\delta}$/YIG and also in Pt/SiO_2 with different level of Fe doping. Because the spin Hall angles of Pt and Ta are opposite in signs [14], we can continuously tune the effective spin Hall angle of the $Pt_{\delta}Ta_{1-\delta}$ alloy from positive, crossing zero, to negative. Most interestingly, both the angular dependent MR at low field and high field disappear simultaneously when the spin Hall angle crosses zero in $Pt_{0.32}Ta_{0.68}$/YIG, evidencing the importance of spin-orbit coupling. While Pt/SiO_2 itself exhibits no obvious feature, an angular dependent MR with $R_{||} \approx R_{\perp} > R_T$ can be reproduced when Pt film or SiO_2 substrate is doped with even tiny amounts of Fe impurity. The observed MR ratio in Pt/SiO_2 increases almost linearly with Fe dopant in SiO_2 substrate at temperatures between 10 K and 300 K. These identify that magnetic scattering is also a key factor to produce this unique MR at high field. Therefore，by complete control of composition, magnetic field strength and orientation as well as temperature, we demonstrate both spin-orbit coupling and magnetic scattering are crucial to produce high-field magnetoresistance.

We use *rf* magnetron co-sputtering to deposit amorphous SiO_2 (with or without Fe dopants) onto the thermally oxidized Si(001) substrates. *Dc* magnetron sputtering co-deposition is utilized to grow 3-nm $Pt_{\delta}Ta_{1-\delta}$ alloy with different δ onto polished polycrystalline YIG and Fe-doped amorphous SiO_2 substrates with roughness of ~0.3 nm [23]. Both *dc* and *rf* magnetron sputtering are performed at room temperature. And the relative composition in $Pt_{\delta}Ta_{1-\delta}$ alloy and SiO_2(Fe) are controlled by changing the deposition rate of sputtering sources. The deposited thin films have been patterned into

Hall bars of width 0.2 mm with one long segment (5 mm) and three pairs of short side bars 1.5 mm apart as shown in Fig. 1(a). And the 4-terminal method was used to measure the MR with current along the long segment and voltage from the two side bars. In order to access the angular dependence of MR, we rotate the magnetic field H within the xy, xz, and yz planes with angles ϕ_{xy}, α_{xz}, and θ_{yz} relative to x, x, and z axis respectively. For the thermal measurements, a perpendicular temperature gradient of $\nabla_z T \approx 20$ K/mm is established by placing the sample in between, and in contact with, two large Cu plates maintained at different constant temperatures. Under a vertical temperature gradient, the spin Seebeck effect in YIG drives a pure spin current flow along the z direction and can be detected as a thermal voltage V_{th} via the ISHE with $\boldsymbol{E}_{ISHE} \propto \theta_{SH} \boldsymbol{J}_S \times \boldsymbol{\sigma}$ in the $Pt_\delta Ta_{1-\delta}$ layer. Where, θ_{SH} denotes the spin Hall angle of $Pt_\delta Ta_{1-\delta}$ alloy, $\boldsymbol{J}_S$ and $\boldsymbol{\sigma}$ are the flow directions of spin current and spin index respectively, and $\boldsymbol{\sigma}$ is parallel to YIG magnetization direction. The distance between the two voltage leads for measuring the thermal voltage is ~4.2 mm.

Figure 1(b) presents the field dependence of $R_{||}$ (black square) and R_T (red circle) for Pt(3 nm)/YIG with in-plane field below 10 mT. Pt(3 nm)/YIG exhibits a sizable MR with $R_{||} > R_T$, which can be described by the SMR model. The small plateau near the origin is commonly found in thick YIG substrates [24-26]. The different widths of $R_{||}$ and R_T is due to the shape of the rectangular YIG substrate, which is absent in a square YIG substrate [10]. In Fig. 1 (b), the blue triangle (right scale) shows the thermal voltage V_{th} for Pt(3 nm)/YIG under a vertical temperature gradient, where H is applied along y axis (ϕ_{xy}=90°). Both the V_{th} and R_T, having the same saturation field along the transverse direction, are thus clearly correlated. The asymmetric signal in field with a magnitude of ~16 μV is

consistent with ISHE ($\boldsymbol{E}_{ISHE} \propto \boldsymbol{J}_S \times \boldsymbol{\sigma}$), with negligible contribution from anomalous Nernst effect of possible polarized Pt [27-29]. Since MR/ V_{th} is a symmetry/anti-symmetric with magnetic field respectively, magnetization distribution under $+H_0$ and $-H_0$ would give the same resistance but opposite V_{th}. Therefore, MR exhibits no hysteresis while the SSE shows large hysteresis in the low-field range. As Ta is less than half filled and Pt is more than half filled, their spin Hall angle should have opposite signs. Consistently, we observe an opposite field dependence of V_{th} (blue triangle right scale) for Ta(3 nm)/YIG in Fig. 1(c). This is also consistent with the prediction of *ab initio* calculation and observation in other reports [14, 30-32]. Since SMR is proportional to the square of spin Hall angle, Ta(3 nm)/YIG exhibits similar angular dependent resistance as that of Pt(3 nm)/YIG with $R_{||}>R_T$ [Fig. 1(c)], albeit with different magnitude.

Our measurements clearly show that the sign of spin Hall angle of Pt is opposite to that of Ta. Thus it provides an interesting venue to manipulate and tailor the effective spin Hall angle of $Pt_\delta Ta_{1-\delta}$ alloy by controlling the relative composition. Indeed, V_{th}, which is proportional to the spin Hall angle, increases monotonically from -4 μV to +16 μV with increasing Pt content as shown in Fig. 2(a). The sign changes at δ=0.32, possessing essentially zero spin Hall angle. Concurrently, as shown in Fig. 2(b), the MR ratio obtained at 10 mT also approaches zero in $Pt_{0.32}Ta_{0.68}$(3 nm)/YIG, indicating that the low field MR is directly related to pure spin current, consistent with the SMR model. Altering the Pt content in either way would increase the absolute value of spin Hall angle, thus increasing the MR ratio.

Since the first observation of the MR in Pt/YIG, controversy has existed whether the magneto-transport behavior was due to pure spin current related effect or induced

moment. Tuning the spin Hall angle in $Pt_{\delta}Ta_{1-\delta}$ alloy gives us advantage to separate the contribution from spin-orbit coupling and possible induced moment, which are typically entangled in Pt/YIG structure. Thus, it would be interesting to examine the MR behavior in $Pt_{0.32}Ta_{0.68}$ at high field where the spin Hall angle is essentially zero. Both in-plane resistances for Pt(3 nm)/YIG and Ta(3 nm)/YIG have $\sin^2\phi$ angular dependence when the magnetic field is rotating in *xy* or *yz* plane, but the MR ratios increase strongly with magnetic field as shown in Fig. 3(a) and 3(b) ($\Delta R/R$ keeps increasing up to 16 T without any signature of saturation, not shown). The increase is particularly strong for Ta(3 nm)/YIG, $\Delta R/R$ enhances by more than one order's magnitude when magnetic field is increased from 0.15 T to 8 T. The drastic increase of MR ratio of Ta/YIG is not well understood yet, and deserves further investigation. In sharp contrast, the MR ratio is gravely suppressed in $Pt_{0.32}Ta_{0.68}$(3 nm)/YIG by ~50 times compared with that of Pt(3 nm)/YIG or Ta (3 nm)/YIG, evidencing the importance of spin-orbit coupling and irrelevance to the induced magnetic moment at interface. Fig. 3(d) and Fig. 3(e) present the temperature dependent AHE of Pt(3 nm)/YIG and Ta(3 nm)/YIG respectively. The AHE of Pt(3 nm)/YIG increases with decreasing temperature and changes sign at around 100 K, and the AHE of Ta(3 nm)/YIG decreases with decreasing temperature, consistent with previous observations [10, 33]. Interestingly, we find the AHE of $Pt_{0.32}Ta_{0.68}$(3 nm)/YIG is also strongly suppressed. Although a theoretical model which can describe the temperature dependent AHE of Pt/YIG and Ta/YIG is still missing, our work clearly demonstrates the key role of spin-orbit coupling since AHE vanishes in $Pt_{\delta}Ta_{1-\delta}$ alloy with zero spin Hall angle. With decreasing temperature, the spin Hall angle and/or spin diffusion length for Pt and Ta would change accordingly. We observe detectable AHE

signal for $Pt_{0.32}Ta_{0.68}$(3 nm)/YIG below 100 K, illustrating the emergence of an appreciable spin Hall angle.

Above results demonstrate the importance of spin-orbit coupling for the angular dependent MR at high field and AHE. In the following, we will further demonstrate that the magnetic scattering source is also critical for the magneto-transport behavior. Figure 4(a) presents the XPS survey of a *clean* SiO_2 substrate with usual elements noted, no trace of magnetic impurities. In a sample of 3-nm *clean* Pt on *clean* SiO_2 substrate, there is neither detectable AHE-type signal [purple curve in Fig. 4 (c)] and nor MR within *xy*-plane [Fig. 4 (b) lower panel], even at 10 K. These results are consistent with those of previous reports. That is, Pt, a strong spin-orbit coupling material, in isolation would not exhibit any unusual features [10, 34, 35]. Using co-deposition technique, we purposely introduce Fe doping into SiO_2 substrate. Clear Fe^{3+}-2p peaks appear in the highly doped range [orange and blue curves in Fig. 4 (a)] [36], where the characteristic peaks of Fe and Si are used to calculate the relative atomic percentage as SiO_2(15.3%Fe) and SiO_2(9.9%Fe) respectively. However, when SiO_2 is lightly doped, no signal of Fe can be detected from XPS analysis [red curve in Fig. 4 (a)]. We estimate the atomic percentage as around SiO_2(0.5%Fe) from our calibrated deposition rate. Remarkably, even with such a small amount of Fe impurity in SiO_2 substrate, Pt(3nm)/SiO_2(0.5%Fe) exhibits a temperature dependent anomalous Hall signal. The R_{AHE} of Pt(3 nm)/SiO_2(0.5%Fe) essentially a constant above 10 K, changes sign and shows large enhancement at 10 K. Note that the R_{AHE} for Pt(3 nm)/SiO_2(0.5%Fe) above 10 K as well as 3-nm *clean* Pt on *clean* SiO_2 substrate have been magnified 5 times for clarity. Meanwhile, an angular dependent MR around 8.7E-6 with $R_{\parallel} \approx R_{\perp} > R_T$ is detected in Pt(3nm)/SiO_2(0.5%Fe) at

300 K [Fig. 4 (b) upper panel] , which increases to 4.0E-5 at 10 K. Therefore, strong spin-orbit coupling in Pt itself would not result in angular dependent MR or AHE-type signal; Magnetic scattering source, *i.e.*, Fe impurity in SiO_2 substrate for Fig. 4 is also crucial. And we find the transition temperature of AHE in Pt/SiO_2(Fe) increases with increasing Fe doping level [23]. Similar behavior has also been reported in Pt/$LaCoO_3$ system, where the AHE-type signal and unconventional MR only emerge below the Curie temperature of $LaCoO_3$ substrate [35]. Our findings are in contrast to the recently proposed Hanle magnetoresistance model, where Pt itself, with strong spin-orbit coupling, exhibits angular dependent MR under magnetic field [20]. In Ref. 20, the angular dependent MR (in the order of 1E-5) exists only in part of the nominal same samples, suggesting that the potential magnetic contamination should be carefully excluded. Our experimental findings demonstrat that XPS only is not sufficient for this purpose.

Figure 4(d) presents the MR ratio dependence on the Fe doping in SiO_2 substrate at different temperatures between 10 K and 300 K. The MR ratio monotonically increases with Fe doping within the entire temperature range. For a given sample, the MR ratio also increases unabated with decreasing temperature since the magnetic-related scattering is expected to increase when the temperature decreases. We note, even for the highly doped SiO_2(15.3%Fe), the substrate is still insulating; The peculiar angular dependence at room temperature also shows that it is not the conventional AMR [Fig. 4(b)]. In addition, the angular dependent MR and AHE-type signal can also be reproduced when Pt film itself is doped with small amount of Fe impurity [Fig. 4(e) and Fig. 4(f)]. We estimate the doping level of Fe in Pt is less than 0.1%. The AHE part is almost zero above 200 K, and

becomes visible at low temperature. And the sign of AHE also changes between 10 K and 50 K, similar as Pt(3 nm)/SiO_2(0.5%Fe) in Fig. 4(c).

Recently, Zhang et. al. derived an angular dependent MR from the combination of spin dependent scattering at interface and spin-orbit coupling [37]. Although the angular dependence of $R_{||} \approx R_{\perp} > R_T$ is not rigorously reproduced in this model, it provides an alternative theoretical approach for the understanding of the new MR in Pt/YIG and related systems. After magnetic substrate has been saturated, the magnetic field would not have distinct influence on the magnetization. Thus, the sharp increase of MR ratio with magnetic field should mostly relate to the spin current in the non-magnetic layer. The magnetic field can either directly change the spin direction (*e.g.,* Hanle effect), or momentum of electron (Lorenz force) which in turn influence spin through spin-orbit coupling. Here, we provide comprehensive experimental data showing that interfacial magnetic scattering and spin direction in spin-orbit material are two important ingredients for theoretical understanding the MR in heavy metal on ferromagnetic insulators, such as Pt/YIG.

In summary, we systematically study the angular dependent MR in $Pt_{\delta}Ta_{1-\delta}$ alloy on YIG and Fe doped-SiO_2 substrates. Through the composition variation, the spin Hall angle of $Pt_{\delta}Ta_{1-\delta}$ alloy can be continuously engineered from positive, crossing zero, to negative. In Pt/SiO_2 (where the magnetic scattering at the interface is absent) and $Pt_{0.32}Ta_{0.68}$/YIG (where the spin Hall angle is zero), the angular dependent MR at both low field and high field and the AHE all disappear. In addition, the MR ratio of Pt/SiO_2 (Fe doped) increases monotonically with doping level at all temperatures between 10 K

and 300 K. We thus identify both the spin-orbit coupling and magnetic scattering as the essential elements to acquire the intriguing magneto-transport behavior.

Acknowledgements

This work was supported by the National Natural Science Foundation of China (Grant Nos. 51571109, 51601087, 11374145, and 11304150); the Natural Science Foundation of Jiangsu Province (Grant No. BK20150565). Work at JHU was supported in part by SHINES, an EFRC funded by the US DOE Basic Energy Science under award number SC0012670. We thank Prof. Michel Dyakonov, Prof. Shufeng Zhang, Prof. Weiyi Zhang and Prof. Jiang Xiao for fruitful discussions and High Magnetic Field Laboratory, CAS for the help of PPMS measurements.

Reference:

1. M. N. Baibich, J. M. Broto, A. Fert, F. N. Van Dau, F. Petroff, P. Etienne, G. Creuzet, A. Friederich and J. Chazelas, Phys. Rev. Lett. **61**, 2472 (1988).
2. G. Binasch, P. Grünberg, F. Saurenbach and W. Zinn, Phys. Rev. B **39**, 4828 (1989).
3. T. Miyazaki and N. Tezuka, J. Magn. Magn. Mater **139**, 231 (1995).
4. J. S. Moodera, L. R. Kinder, T. M. Wong and R. Meservey, Phys. Rev. Lett. **74**, 3273 (1995).
5. A. P. Ramirez, J. Phys.: Condens. Matter **9**, 8171 (1997).
6. W. Thomson, Proc. R. Soc. Lond. **8**, 546 (1856).
7. T. R. McGuire and R. I. Potter, IEEE Trans. Magn. **11**, 1018 (1975).
8. R. C. O'Handley, *Modern Magnetic Materials: Principles and Applications*. (Wiley, 1999).
9. M. Weiler, M. Althammer, F. D. Czeschka, H. Huebl, M. S. Wagner, M. Opel, I.-M. Imort, G. Reiss, A. Thomas, R. Gross and S. T. B. Goennenwein, Phys. Rev. Lett. **108**, 106602 (2012).
10. S. Y. Huang, X. Fan, D. Qu, Y. P. Chen, W. G. Wang, J. Wu, T. Y. Chen, J. Q. Xiao and C. L. Chien, Phys. Rev. Lett. **109**, 107204 (2012).
11. Y. M. Lu, J. W. Cai, S. Y. Huang, D. Qu, B. F. Miao and C. L. Chien, Phys. Rev. B **87**, 220409 (2013).
12. H. Nakayama, M. Althammer, Y. T. Chen, K. Uchida, Y. Kajiwara, D. Kikuchi, T. Ohtani, S. Geprägs, M. Opel, S. Takahashi, R. Gross, G. E. W. Bauer, S. T. B. Goennenwein and E. Saitoh, Phys. Rev. Lett. **110**, 206601 (2013).
13. M. Althammer, S. Meyer, H. Nakayama, M. Schreier, S. Altmannshofer, M. Weiler, H. Huebl, S. Geprägs, M. Opel, R. Gross, D. Meier, C. Klewe, T. Kuschel, J.-M. Schmalhorst, G.

Reiss, L. Shen, A. Gupta, Y.-T. Chen, G. E. W. Bauer, E. Saitoh and S. T. B. Goennenwein, Phys. Rev. B **87**, 224401 (2013).
14. C. Hahn, G. de Loubens, O. Klein, M. Viret, V. V. Naletov and J. Ben Youssef, Phys. Rev. B **87**, 174417 (2013).
15. Y.-T. Chen, S. Takahashi, H. Nakayama, M. Althammer, S. T. B. Goennenwein, E. Saitoh and G. E. W. Bauer, Phys. Rev. B **87**, 144411 (2013).
16. J. C. Slonczewski, J. Magn. Magn. Mater **159**, L1 (1996).
17. L. Berger, Phys. Rev. B **54**, 9353 (1996).
18. E. Saitoh, M. Ueda, H. Miyajima and G. Tatara, Appl. Phys. Lett. **88**, 182509 (2006).
19. B. F. Miao, S. Y. Huang, D. Qu and C. L. Chien, Phys. Rev. Lett. **112**, 236601 (2014).
20. S. Vélez, V. N. Golovach, A. Bedoya-Pinto, M. Isasa, E. Sagasta, M. Abadia, C. Rogero, L. E. Hueso, F. S. Bergeret and F. Casanova, Phys. Rev. Lett. **116**, 016603 (2016).
21. T. Lin, C. Tang and J. Shi, Appl. Phys. Lett. **103**, 132407 (2013).
22. M. I. Dyakonov, Phys. Rev. Lett. **99**, 126601 (2007).
23. See the Supplemental Material.
24. Y. M. Lu, Y. Choi, C. M. Ortega, X. M. Cheng, J. W. Cai, S. Y. Huang, L. Sun and C. L. Chien, Phys. Rev. Lett. **110**, 147207 (2013).
25. K.-i. Uchida, T. Nonaka, T. Ota and E. Saitoh, Appl. Phys. Lett. **97**, 262504 (2010).
26. K.-i. Uchida, J.-i. Ohe, T. Kikkawa, S. Daimon, D. Hou, Z. Qiu and E. Saitoh, Phys. Rev. B **92**, 014415 (2015).
27. B. F. Miao, S. Y. Huang, D. Qu and C. L. Chien, AIP Advances **6**, 015018 (2016).
28. T. Kikkawa, K. Uchida, Y. Shiomi, Z. Qiu, D. Hou, D. Tian, H. Nakayama, X. F. Jin and E. Saitoh, Phys. Rev. Lett. **110**, 067207 (2013).
29. T. Kikkawa, K. Uchida, S. Daimon, Y. Shiomi, H. Adachi, Z. Qiu, D. Hou, X. F. Jin, S. Maekawa and E. Saitoh, Phys. Rev. B **88**, 214403 (2013).
30. T. Tanaka, H. Kontani, M. Naito, T. Naito, D. S. Hirashima, K. Yamada and J. Inoue, Phys. Rev. B **77**, 165117 (2008).
31. L. Liu, C.-F. Pai, Y. Li, H. W. Tseng, D. C. Ralph and R. A. Buhrman, Science **336**, 555 (2012).
32. M. Morota, Y. Niimi, K. Ohnishi, D. H. Wei, T. Tanaka, H. Kontani, T. Kimura and Y. Otani, Phys. Rev. B **83**, 174405 (2011).
33. Y. Yang, B. Wu, K. Yao, S. Shannigrahi, B. Zong and Y. Wu, J. Appl. Phys. **115**, 17C509 (2014).
34. B. F. Miao, S. Y. Huang, D. Qu and C. L. Chien, Phys. Rev. Lett. **111**, 066602 (2013).
35. T. Shang, Q. F. Zhan, H. L. Yang, Z. H. Zuo, Y. L. Xie, Y. Zhang, L. P. Liu, B. M. Wang, Y. H. Wu, S. Zhang and R.-W. Li, Phys. Rev. B **92**, 165114 (2015).
36. T. Yamashita and P. Hayes, Appl. Surf. Sci. **254**, 2441 (2008).
37. S. S.-L. Zhang and S. Zhang, J. Appl. Phys. **115**, 17C703 (2014).

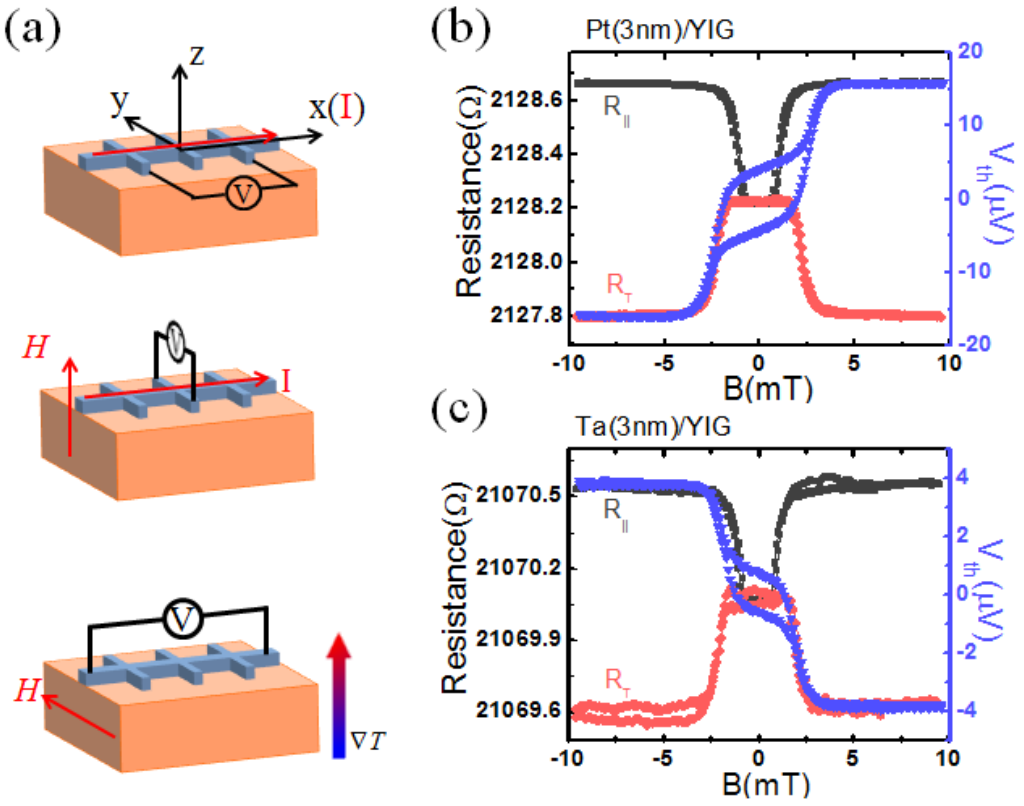

Fig. 1 (a) Schematics for the measurements of magnetoresistance, anomalous Hall effect and thermal voltage V_{th} with temperature gradient long the z axis. Field dependent longitudinal MR $R_{\parallel}$ (black curve), transverse MR R_T (red curve), and thermal voltage V_{th} (blue curve) for (b) Pt(3 nm)/YIG, and (c) Ta(3 nm)/YIG at room temperature.

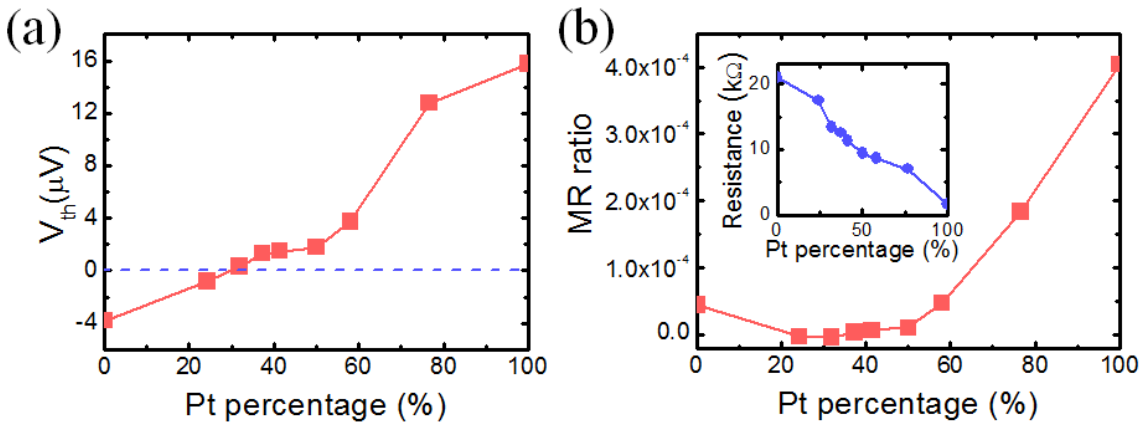

Fig. 2 (a) Thermal voltage V_{th}, and (b) MR ratio for 3nm-$Pt_{\delta}Ta_{1-\delta}$ alloy on YIG substrate with perpendicular temperature gradient at different Pt percentage at room temperature. The insert of (b) presents the dependence of resistance 3nm-$Pt_{\delta}Ta_{1-\delta}$ alloy on Pt component.

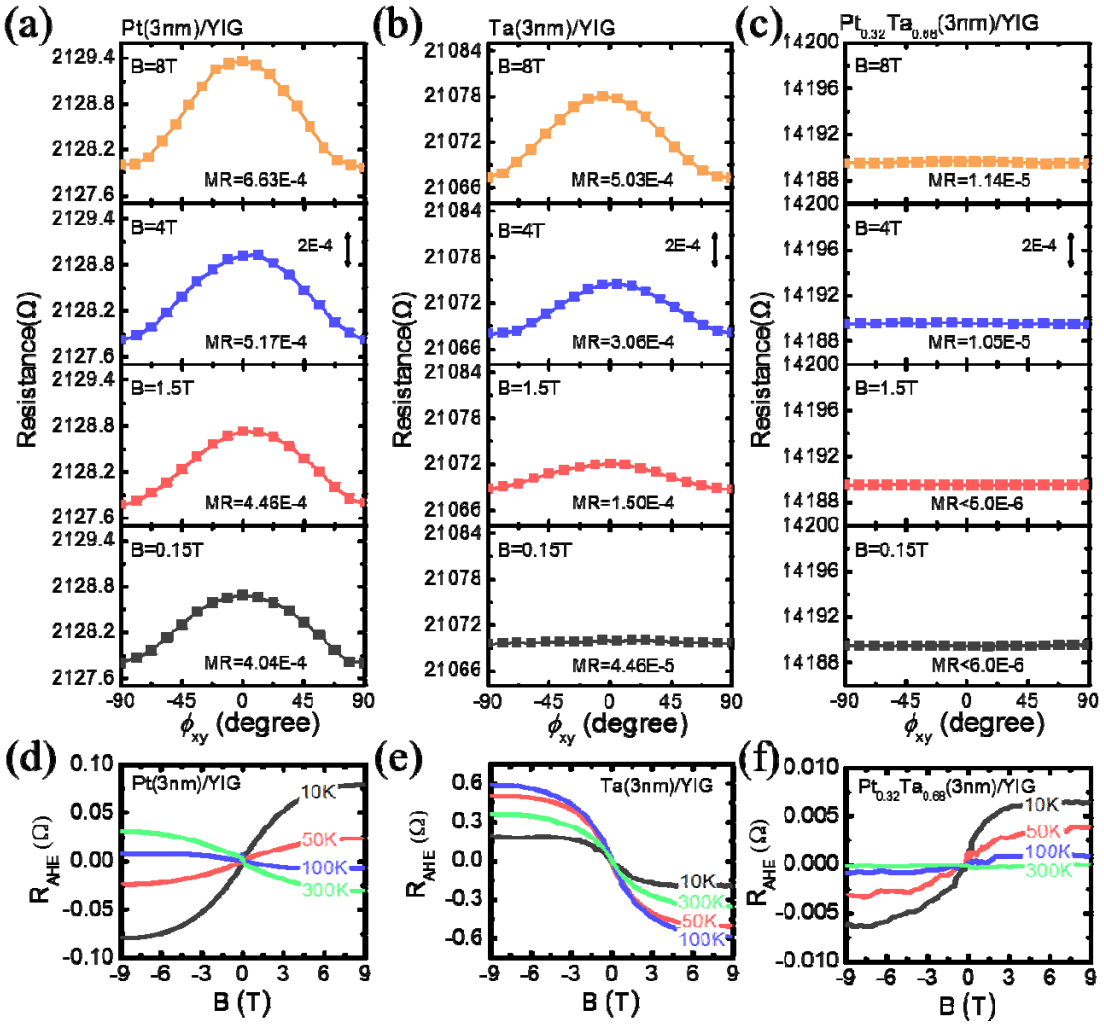

Fig. 3 Room temperature angular dependent MR as a function of ϕ_{xy} for (a) Pt(3 nm)/YIG, (b) Ta(3nm)/YIG, and (c) $Pt_{0.32}Ta_{0.68}$(3 nm)/YIG measured at 0.15 T (black), 1.5 T (red), 4 T (blue) and 8 T (orange) respectively. (d-f) present the temperature dependent AHE for Pt(3 nm)/YIG, Ta(3 nm)/YIG, and $Pt_{0.32}Ta_{0.68}$(3 nm)/YIG, respectively.

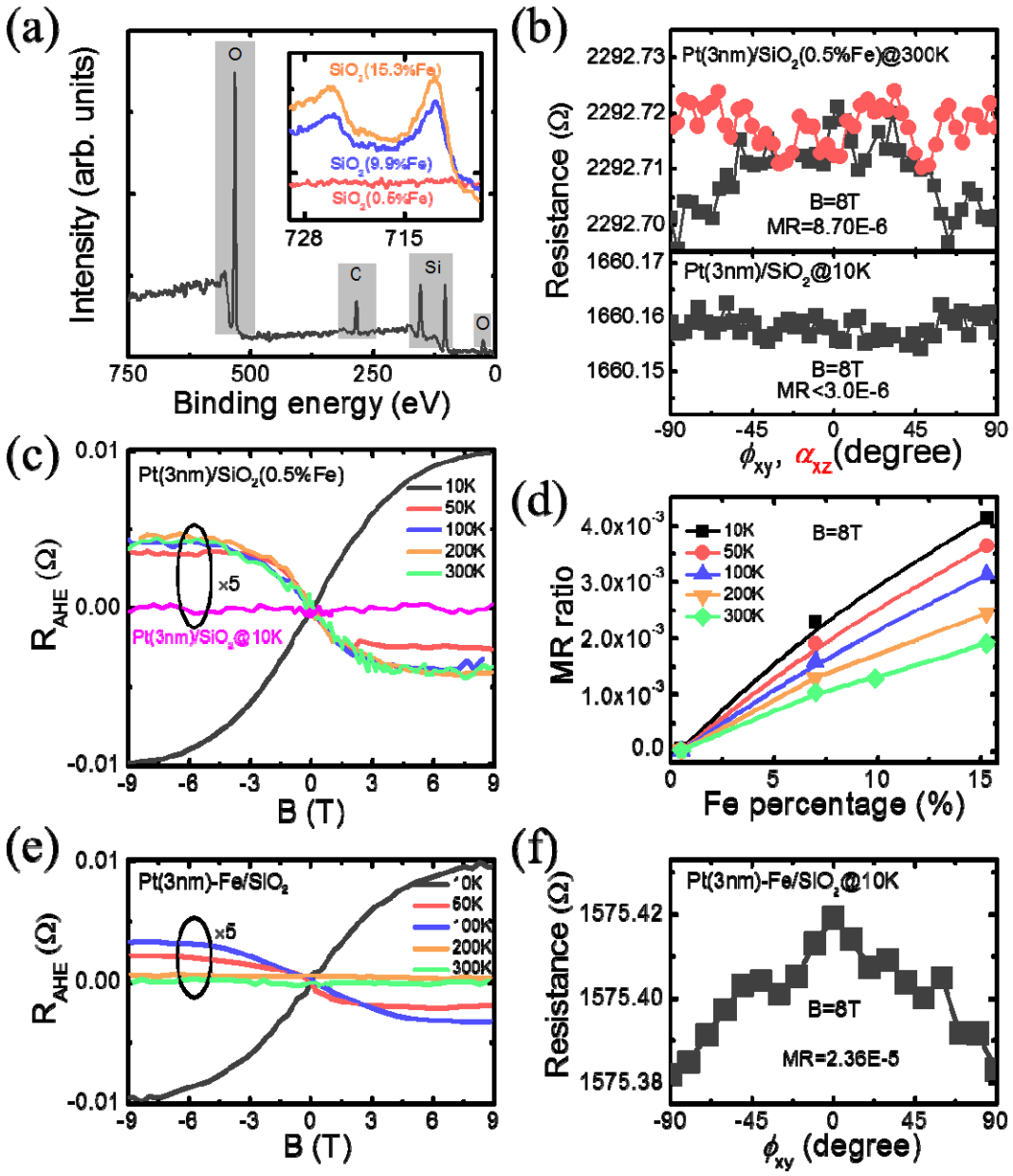

Fig. 4 (a) XPS survey of *clean* SiO_2 substrate. The insert presents the Fe-2p peaks for SiO_2 substrates with different Fe doping percentage. (b) Up panel: angular dependence of MR for Pt(3 nm)/SiO_2(0.5%Fe) in ϕ_{xy} scan (black) and α_{xz} scan (red) measured at 8T and at 300 K; Down panel: angular dependence of MR for 3-nm *clean* Pt on *clean* SiO_2 in ϕ_{xy} measured at 8T and at 10 K. (c) The anomalous Hall resistance for Pt(3 nm)/SiO_2(0.5%Fe) at different temperatures with nominal linear background subtracted. For comparison, we also include the anomalous Hall resistance for 3-nm *clean* Pt on *clean* SiO_2 substrate at 10 K. (d) The MR ratio for 3-nm Pt deposited on SiO_2 substrates at different Fe doping percentage obtained at 8 T and at 300 K. (e) The anomalous Hall resistance for Pt(3 nm)-Fe/SiO_2 at different temperatures with nominal linear background subtracted. (f) Angular

dependence of MR in $\square_{xy}$ scan under 8 T magnetic field and 10K for 3-nm Pt(doped with Fe)/SiO_2.